

CONTROL OF LASER RADIATION PARAMETERS https://doi.org/10.1070/QEL17542

Adaptive system for correcting optical aberrations of high-power lasers with dynamic determination of the reference wavefront

A.V. Kotov, S.E. Perevalov, M.V. Starodubtsev, R.S. Zemskov, A.G. Alexandrov, I.V. Galaktionov, A.V. Kudryashov, V.V. Samarkin, A.A. Soloviev

Abstract. **We present the results of the aberration correction of laser radiation wavefront using a dynamic method for determining the reference wavefront. The method, which is based on the processing of synchronously obtained data on the near- and far-field zones, significantly improves the focusing quality with active wavefront correction, especially under conditions of dynamic aberrations. An increase in the Strehl number S from 0.7 to 0.86 is demonstrated when a beam 18 cm in diameter is focused by an $F/2.5$ parabolic mirror.**

Keywords: *adaptive optical system, deformable bimorph mirror, focusing quality optimisation, dynamic aberrations, consideration of differential aberrations, PEARL laser facility.*

1. Introduction

Achievement of the diffraction limit for the peak intensity of a laser pulse during focusing is limited by distortions of its wavefront. The wavefront is distorted in imperfect optical elements, in elements with a significant thermal load, as well as in air flows. To compensate for wavefront distortions of high-power lasers, use is made of deformable mirrors with a controllable surface shape, which are key elements of adaptive optical systems (AOS's).

In an AOS, feedback to a mirror with a controllable surface shape [1–3] is carried out via a wavefront sensor (WFS) [4] located in the diagnostic optical path. The AOS operating in the active correction regime seeks to give the mirror a shape that minimises the differences between the WFS readings and the reference wavefront. The latter is chosen so as to ensure ideal focusing of radiation in the waist of the focusing system. In the general case, the work of the AOS is therefore divided into two stages: calibration, which involves finding the reference wavefront [5–8], and correction, which involves maintaining this wavefront [9].

A.V. Kotov, S.E. Perevalov, M.V. Starodubtsev, R.S. Zemskov, A.A. Soloviev Institute of Applied Physics, Russian Academy of Sciences, ul. Ulyanova 46, 603950 Nizhny Novgorod, Russia; e-mail: kotov@ipfran.ru, 7oloviev@gmail.com, perevalov@ipfran.ru, zemskov@ipfran.ru, mstar@appl.sci-nnov.ru;
A.G. Alexandrov, I.V. Galaktionov, V.V. Samarkin Institute of Geosphere Dynamics, Russian Academy of Sciences, Leninsky prosp. 38, korpus 1, 119334 Moscow, Russia; e-mail: alex@activeoptics.ru, galaktionov@activeoptics.ru, samarkin@nightn.ru;
A.V. Kudryashov Institute of Geosphere Dynamics, Russian Academy of Sciences, Leninsky prosp. 38, korpus 1, 119334 Moscow, Russia; Moscow Polytechnic University, ul. Bol'shaya Semenovskaya 38, 107023 Moscow, Russia; e-mail: kud@activeoptics.ru

Received 15 February 2021; revision received 1 June 2021
Kvantovaya Elektronika **51** (7) 593–596 (2021)
Translated by E.N. Ragozin

The impossibility of measuring the wavefront of superhigh-power radiation has the result that the diagnostic channel is organised in an attenuated beam behind one of the large-aperture transport mirrors. The radiation in the diagnostic channel passes through the thickness of the mirror, bypassing some of the elements of the working-beam (high-power) path, which leads to the so-called differential distortions that are manifested in the difference between the reference wavefront and the one observed in the plane of WFS location. Calibrating the AOS makes it possible to take into account the differential distortions, which is necessary to maintain high-quality focusing in the correction regime.

Calibration, as a rule, involves an iterative procedure, which consists in optimising the focusing spot by iterating through possible values of the voltages at the control electrodes of the deformable mirror [5–8]. The duration of this procedure is tens of minutes, with the result that the AOS is sensitive to all faster dynamic aberrations. The wavefront is measured at the end of the procedure and its shape is taken as the reference. Errors in determining the wavefront reference obviously impair the quality of focusing during correction.

The correction stage involves applying to the deformable mirror the voltages obtained by decomposing the WFS readings in terms of the response functions of the deformable mirror; this procedure is based on direct algorithms [9] and can be fast enough to compensate for wavefront aberrations in the air flows present in the laboratory [10].

Therefore, modern adaptive systems effectively cope with the task of maintaining a predetermined wavefront profile, but encounter certain difficulties in finding its reference wavefront, which depends on the differential distortions in the diagnostic path and focusing system.

In this work, for the first time, as far as the authors know, an approach is proposed for the dynamic determination of the reference wavefront profile, which relies on the processing of synchronously obtained data from the Shack–Hartmann sensor (near-field zone) and the image of the laser beam waist (far-field zone). This approach makes it possible to significantly improve the accuracy and reduce the focal-spot optimisation time due to correct interpretation of the contribution of dynamic aberrations.

2. Experiment

The proposed approach was implemented in the course of modifying a 240-mm adaptive wavefront correction system (Active Optics NightN Ltd, Russia) [11] on the PEARL laser facility [12, 13] and made it possible to demonstrate in laboratory conditions an increase in the Strehl number up to S =

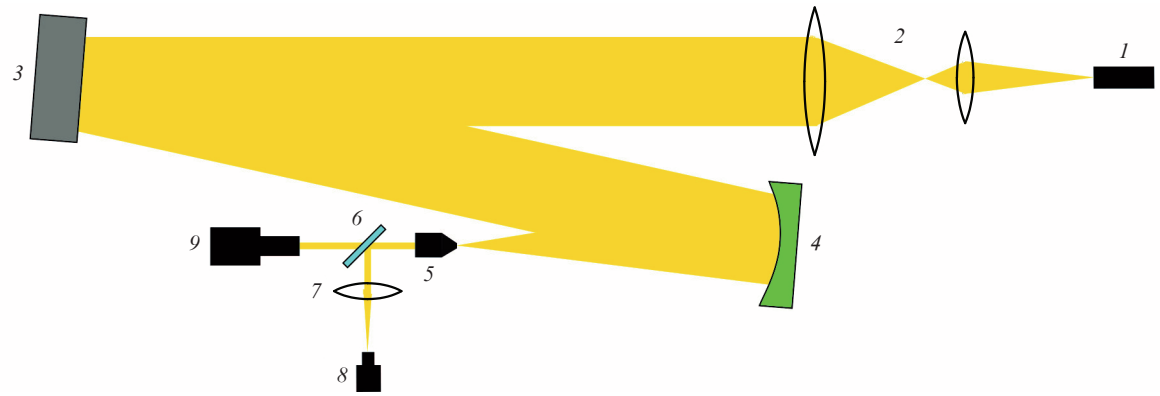

Figure 1. Schematic of the experiment: (*1*) laser diode; (*2*) expanding telescope; (*3*) deformable mirror; (*4*) *F*/2.5 off-axis parabolic mirror; (*5*) microscope objective; (*6*) beam splitter; (*7*) lens with a focal length $f = 180$ mm; (*8*) far-field camera; (*9*) WFS.

0.86 for laser diode radiation when focusing a laser beam 180 mm in diameter by an *F*/2.5 off-axis parabolic mirror.

The optical configuration for the experimental demonstration of the effectiveness of the approach is schematically shown in Fig. 1.

The laser beam 180 mm in diameter was made by expanding the beam of a cw laser diode (Thorlabs, LP915-SF40, wavelength: $\lambda = 915$ nm) in a telescope. Use was made of a 96-electrode deformable bimorph mirror optimised for a beam with a diameter of 200 mm. The design and capabilities of the bimorph mirror are described in detail in Ref. [13]. The requisite shape of the wavefront profile was maintained using the phase conjugation algorithm described in Ref. [14]. For the working range of spatial frequencies of aberrations, the phase conjugation provided the root-mean-square deviation (RMSD) σ of the measured wavefront from the reference one under $\lambda/20$ and compensated for phase distortions when the adaptive correction system was operating at a frequency of at least 5 Hz. Focusing was carried out with an *F*/2.5 off-axis parabolic mirror, which in the limit provided a diffraction spot 3.34 μm in diameter at the $1/e^2$ intensity level. The radiation diverging from the waist was collimated by a microlens with NA = 0.65. Then, after being reflected from the beam splitter, it was focused by a lens ($f = 180$ mm) onto the far-field camera. Part of the beam that passed through the beam splitter fell on the Shack–Hartmann sensor [4]. Parabolic mirror *4* together with objective *5* provided optical conjugation of the surface planes of the bimorph mirror and the lenslet array of the Shack–Hartmann sensor, whose accuracy was 5–10 nm. Focusing was carried out in the target chamber of the PEARL laser-plasma facility using large-aperture optical elements. To do this, the radiation of the laser diode was introduced into the high-power optical path. The resultant AOS calibration can be used to correct the wavefront of femtosecond pulses of the PEARL laser at full power.

In the correction system under description, there were dynamic aberrations of the radiation wavefront arising from nonstationary air flows between telescope *2* and deformable mirror *3*. As a result, the readings of the Shack–Hartmann sensor contained a random two-dimensional component with σ_d up to 30 nm and a characteristic spatial scale of 0.25 of the aperture, which completely changed in a characteristic time of the order of 1 s. In this case, there were no significant variations in the amplitude profile of the radiation. The amplitude of the dynamic aberrations could be controlled by blocking the air flows. In addition, air flows were completely eliminated in the parts of the configuration path located after the deformable mirror.

Under ideal conditions, for a round spatially uniform laser beam whose size is matched to the active size of the mirror, σ is about 20 nm when dynamic aberrations are blocked. For an unmistakably determined wavefront reference, this corresponds, according to the Marechal approximation, to the Strehl number $S > 0.95$ [15]. In our experiment, the S values calculated from the images from the focal camera were usually lower (see Table 1), which is explained by errors in determining the wavefront reference and the contribution of dynamic aberrations. The Strehl number S, as in Ref. [13], was calculated taking into account the intensity distribution in the near-field zone of radiation.

Table 1. Strehl number S and RMSD σ, which were determined by different methods in the case of active phase conjugation, in relation to the amplitude of dynamic aberrations σ_d caused by air flows.

Method	$\sigma_d = 30$ nm	$\sigma_d = 15$ nm
1	$S < 0.2$; $\sigma = 25$ nm	$S = 0.3$; $\sigma = 20$ nm
2	$S = 0.55$; $\sigma = 25$ nm	$S = 0.7$; $\sigma = 20$ nm
3	$S = 0.86$; $\sigma = 25$ nm	$S = 0.86$; $\sigma = 20$ nm

3. Wavefront correction

The wavefront was corrected using the phase conjugation algorithm [9]. In this case, the reference wavefront was determined by three different methods. These are method 1 – hill-climbing algorithm by electrode voltages [14], method 2 – hill-climbing algorithm by linear combinations of electrodes corresponding to Zernike modes [16, 17], and method 3 based on the original dynamic method for determining the reference, whose description is the main subject of this paper.

Method 3 is based on the gradient descent algorithm, but, unlike methods 1 and 2, in which the focal spot is optimised by iterating through possible values of the control voltages at the electrodes of the deformable mirror, method 3 iterates through possible wavefronts. If the focal spot improves in the course of wavefront variation, then the corresponding wavefront is taken as the reference one, after which a new variation is performed, and so on until the cycle is exited. Variations of the wavefront in the form of Zernike modes (by analogy with Ref. [17]) were carried out using the deformable mirror. To implement the

method, it is necessary to have the technical ability to simultaneously capture (read out) images from the focal camera and from the Shack–Hartmann sensor. Methods 1 and 2 do not use Shack–Hartmann sensor readings.

The main disadvantage of methods 1 and 2 is the assumption that the electrode voltages are uniquely related to the wavefront. However, this is not the case with dynamic aberrations. Dynamic aberrations add up with variations in the shape of the mirror and blur the effect of changing voltages at the electrodes. The accuracy of determining the reference front at this becomes lower.

By contrast, method 3 measures the wavefront variations directly, with the result that dynamic aberrations do not affect the accuracy of the method in any way. Therefore, the main advantage of method 3 is the correct treatment of dynamic aberrations. Note that these conclusions are valid only in the absence of a dynamic component in the difference aberrations.

It is noteworthy that dynamic determination of the reference wavefront profile is possible even in the absence of an expensive element with a controllable surface shape. To do this, the variations of the near- and far-field zones that arise exclusively due to dynamic aberrations are processed synchronously. This circumstance may be used as an alternative method for measuring differential distortions in an optical configuration.

4. Analysis of experimental data

The correction results for different methods of finding the reference profile are shown in Table 1. Here σ is the RMSD of the measured wavefront from the reference one in the case of active correction, and σ_d is the time-averaged RMSD of the wavefront from its mean value for fixed voltages on the deformable mirror. In methods 2 and 3, optimisation was carried out according to the first eleven Zernike modes in the nomenclature of Ref. [18].

It follows from Table 1 that the accuracy of finding the reference profile by method 3 is significantly higher than by methods 1 and 2. Furthermore, method 3 is less affected by dynamic aberrations. The superiority of method 3 over method 2 at lower σ_d is achieved by correct inclusion of the hysteresis and linear dependence of the electrodes. One can also see from Table 1 that the efficiency of active correction slightly deteriorates for stronger dynamic aberrations: σ becomes larger regardless of the method for finding the reference profile.

Typical far-field patterns for the reference wavefront profiles determined by different methods are shown in Fig. 2. In all these cases, correction was performed using the phase conjugation algorithm.

5. Main results

1. A method for dynamic determination of the reference wavefront for adaptive correction of the wavefront in high-power laser systems is proposed. The method is based on the analysis of synchronously obtained data on the near- and far-field zones, allows us to correctly interpret dynamic aberrations and take into account the limitations of the deformable mirror associated with the hysteresis and nonlinearity of electrodes.

2. In comparison with the alternative methods considered above, the proposed dynamic method is more precise and requires fewer iterations in the presence of dynamic aberrations caused by air flows.

3. For the bimorph mirror used, method 1 (hill-climbing by variation of control voltages) gives an inaccurate result due to the existence of local maxima of the axial brightness, which for the algorithm are indistinguishable from the global maximum. The use of linearly independent functions – Zernike modes – permits avoiding problems with the local maxima. Since Zernike modes are better suited for describing optical aberrations than mirror response functions, an approximation with a relatively small number of modes is sufficient to effectively compensate for wavefront distortions; therefore, the proposed dynamic method is also based on parametrising the wavefront through the expansion in Zernike modes. In this sense, the results of our studies amply bear out the conclusions of Ref. [17].

4. The processing of synchronously obtained data in the near- and far-field zones makes it possible to search for a reference wavefront profile even in the absence of an element with a controllable shape by analysing dynamic aberrations.

Acknowledgements. The work was supported by Russian Science Foundation [Grant Nos 20-62-46050 (conceptualisation, algorithmisation, and experimental demonstration of the dynamic method) and 20-69-46064 (AOS program code modification)].

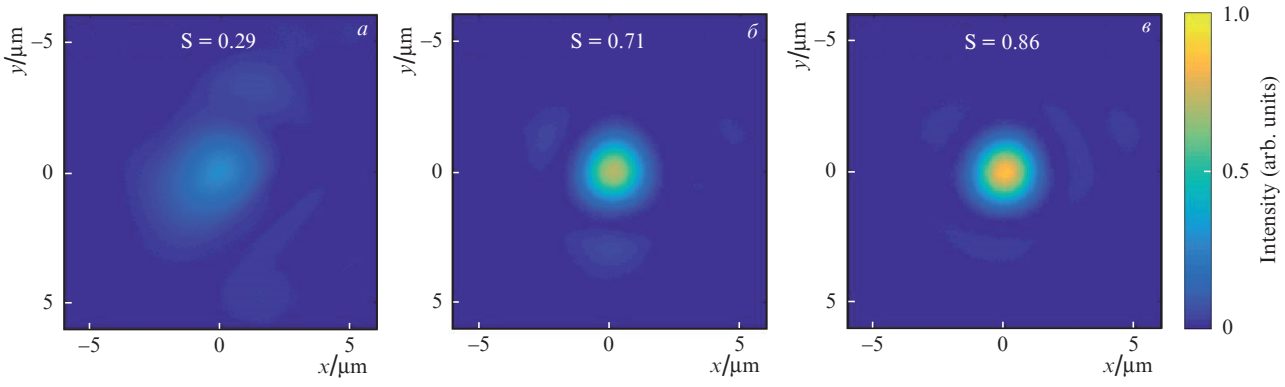

Figure 2. (Colour online) Far-field intensity distributions and Strehl numbers S in the phase conjugation relative to the reference wavefront determined by methods (a) 1, (b) 2 and (c) 3.

References

1. Samarkin V.V., Aleksandrov A.G., Jitsuno T., Romanov P.N., Rukosuev A.L., Kudryashov A.V. *Quantum Electron*., **45** (12), 1086 (2015) [*Kvantovaya Eletro*n., **45** (12), 1086 (2015); https://doi.org/10.1070/qe2015v045n12abeh015961.
2. Toporovsky V. et al., in *High Power Lasers for Fusion Research V*. Ed. by C.L. Haefner, A.A. Awwal (San Francisko, Cal.: SPIE, 2019) p. 1019809; doi: 10.1117/12.2510144.
3. Lefaudeux N. et al. *Nucl. Instrum. Methods Phys. Res. A*, **653**, 164 (2011); doi: 10.1016/j.nima.2010.12.117.
4. Aleksandrov A.G. et al. *Quantum Electron.*, **40**, 321 (2010) [*Kvantovaya Elektron.*, **40**, 321 (2010)]; doi: 10.1070/QE2010v040n04ABEH014061.
5. Sheldakova J.V., Rukosuev A.L., Kudryashov A.V., in *Laser Resonators and Beam Control VII.* Ed. by A.V. Kudryashov (San Jose, Cal.: SPIE, 2004) pp 106–111; doi:10.1117/12.538446.
6. Yang P. et al., in *Proc. 3rd International Symposium on Advanced Optical Manufacturing and Testing Technologies: Optical Test and Measurement Technology and Equipment.* Ed. by J. Pan, J.C. Wyant, H.Wang (Chengdu, China: SPIE, 2007) p. 672303; doi: 10.1117/12.782681.
7. Piatrou P., Roggemann M. *Appl. Opt.*, **46**, 6831 (2007); doi: 10.1364/AO.46.006831.
8. El-Agmy R., Bulte H., Greenaway A.H., Reid D. *Opt. Express*, **13**, 6085 (2005); doi: 10.1364/OPEX.13.006085.
9. Fernández E.J., Iglesias I., Artal P. *Opt. Lett.*, **26**, 746 (2001).
10. Kudryashov A. et al. *Opt. Express*, **28**, 37546 (2020); doi: 10.1364/OE.409201.
11. Kudryashov A. et al. *Proc. SPIE*, **11672**, 116720V (2021); doi: org/10.1117/12.257870.
12. Soloviev A. et al. *Sci. Rep.*, **7**, 12144 (2017); doi: 10.1038/s41598-017-11675-2.
13. Solov'ev A.A. et al. *Quantum Electron.*, **50**, 1115 (2020) [*Kvantovaya Elektron.*, **50**, 1115 (2020)]; doi:10.1070/QEL17446.
14. Kudryashov A.V. et al. *Optoelectron. Instrum. Data Process.*, **48**, 153 (2012); doi:10.3103/S8756699012020070.
15. Born M., Wolf E. *Principles of Optics* (Cambridge: University Press, 1997) Ch. 9.1.3, p. 464, Eqn (24).
16. Yang P., Ao M., Liu Y., Xu B., Jiang W. *Opt. Express*, **15**, 17051 (2007); doi:10.1364/OE.15.017051.
17. Liu Y., Ma J., Li B., Chu J. *Opt. Eng.*, **52**, 016601 (2013); doi:10.1117/1.OE.52.1.016601.
18. Wyant James C., Katherine Creath. *Appl. Opt. Opt. Eng.*, **11**, 28 (1992).